Waveform and discrete LiDAR effective LAI estimates: sensitivity analysis

Karolina D. Fieber [1], Ian J. Davenport[2], James M. Ferryman[1], Robert J. Gurney[2], Mihai A. Tanase[3], Jeffrey P. Walker[4], Jorg M. Hacker[5]

[1] University of Reading, School of Systems Engineering, Whiteknights, Reading, RG6 6AY, UK (k.fieber@pgr.reading.ac.uk, j.m.ferryman@reading.ac.uk)
[2] University of Reading, School of Mathematical and Physical Sciences, Harry Pitt Building, Reading, RG6 6AL, UK ([i.j.davenport, r.j.gurney]@reading.ac.uk)
[3] University of Melbourne, Parkville, Melbourne, 3010 VIC, Australia (mtanase@unimelb.edu.au)
[4] Monash University, Department of Civil Engineering, Clayton, VIC 3800, Australia (jeff.walker@monash.edu)
[5] Airborne Research Australia, School of the Environment, Flinders University, Adelaide, SA 5001, Australia (jmh@flinders.edu.au)

Paper Number: SL2013-018

Abstract

This study has investigated how average effective leaf area index (LAI_e) derived from full-waveform and discrete LiDAR data changes depending on the size of the grid used, over a 150 m by 80 m area of orange orchard. The full-waveform data, acquired with RIEGL LMS-Q560, were decomposed and optimized with a trust-region-reflective algorithm using a custom decomposition procedure focused on extracting denser vegetation point clouds. LiDAR effective LAI (LAI_e) estimates were derived in two ways: (1) from the probability of discrete pulses reaching the ground without being intercepted (discrete point method) and (2) from raw waveform canopy height profile processing adapted to small-footprint laser altimetry (waveform method). The LAI_e estimates for the orange orchard were derived for the whole site as well as in various decreasing grid cell sizes. The discrete point method provided estimates that were 5-10% higher than those of the waveform method, and this difference increased with the decreasing grid cell size. The only exception was the smallest grid (2.5 m) for which the relation was opposite. This was due to the discrete method being limited by the point density. Furthermore, percentage of vegetation cover in the test area was estimated based on aerial photography, and used to derive an average single tree effective LAI depending on the grid cell size. Consequently, to test the effects of vegetation discontinuity on LAI estimation the values of LAI_e for the whole site were simulated based on a set of increasing single orange tree LAI_es (from 0.2 to 5 with 0.2 increments) and known vegetation cover in the test area. This was done by predicting the LAI_e of the orange tree covered area and averaging it with the LAI_e of the bare soil area (LAI_e=0). These 'average' LAI_e values were compared to the 'overall' LAI_es calculated for the whole site from summed probabilities of penetration for the orange tree area and ground area (P_{gapG}=1). As expected, with the increasing LAI_e of a single tree, the area LAI_e increased as well. However, as the LAI_e of single tree increased, the difference between the 'average' LAI_e values and the 'overall' LAI_e values increased significantly, from 5% for a single tree LAI of 0.2 to 73% for a single tree LAI_e of 5.0, showing underestimation of LAI_e by the latter method. The LiDAR LAI_e estimates for the whole study area (simulated large-footprint laser system) differed to those computed as the mean LAI_e value in a 5m by 5 m grid by 14% with the latter estimates agreeing well with simulated LAI_e values of the whole area when the 'average' approach was used (mean single tree LAI_e of 1.6).

1. Introduction

Leaf area index (LAI), vegetation biomass, and canopy height are very important structure parameters for many bio-geoscience applications, such as radiation transfer and carbon balance models. The estimation of LAI sill remains problematic, though, especially at larger scales (Breda, 2003). The remote sensing ways of LAI estimation provide so-called effective leaf area index (Black *et al.*, 1991) (LAI_e) which includes the contributions of woody elements of the canopy. Furthermore, deviation of canopy elements from assumed random distribution (clumping) causes underestimation of LAI from remote sensing methods. The clumping has been reported to occur at several scales: between plants/trees, between branches and between shoots (Breda, 2003). Several studies have proposed methods to correct the LAI estimates from indirect (remote sensing) measurements for clumping effects (Chen *et al.*, 1997; Lang and Yueqin, 1986). For discontinuous and heterogeneous canopies such as rows of crops the underestimation of effective LAI is especially pronounced (Breda, 2003). Lang and Yueqin (1986) proposed a logarithmic averaging technique to account for gaps between rows of sorghum and wheat. Leaf area of crops was measured by averaging the transmission of direct sunlight linearly over a small horizontal distance and taking the logarithm of this mean. This method of LAI estimation provided better results than taking the mean of the transmission over the full distance. This study presents an analogical procedure to that of Lang and Yueqin (1986) for effective LAI estimation from full-waveform small-footprint LiDAR data. The effect of different grid cell size on effective LAI estimation of the whole study area is illustrated using example of orange tree orchard. Furthermore, a simulation of differences in the LAI estimation, when (i) LAI_e is calculated as the mean of LAI_e of the area covered with trees and area of bare and (ii) when LAI_e is computed from summed probabilities of penetration for the orange tree area and ground area.

2. Study area

The study area is located near the town of Yanco, within the Murrumbidgee catchment, New South Wales, Australia. An area of 150 m by 80 m of orange orchard located between 55393360 m and 55393610 m (Easting) and between 6169330 m and 6169250 m (Northing) (UTM, zone 55H) was selected as the test site for this study (Figure 1). Ground elevation ranges from 122 m to 126 m across the site, with the lowest elevations in the North West corner and rising towards the South. The orange trees are denser and taller in the South East while being small and sparse in the North West. The direction of orange tree rows is South West to North East (at about 60^o angle from the North) and the rows are about 7 m apart.

Figure 1. Areas of interest

3. Data

The laser scanning data was acquired by Airborne Research Australia on November 3rd 2006 with a full-waveform Riegl LMS-Q560 instrument (RIEGL, 2012) operating at 1550 nm

wavelength from a light aircraft. The flying altitude was 500 m above the ground level, resulting in a 0.25 m footprint size and average point spacing of 3.2 points/m^2. Both transmitted and received waveforms were recorded and sampled with a frequency of 1GHz (1 ns spacing). The laser altimetry data was captured along a 75 km-long transect line across the Yanco site. It was then extracted using the GeoCodeWF commercial software.
The aerial photography was taken using an 11MegaPixel Canon EOS-1Ds digital camera fitted with a 34 mm lens, mounted on the same aircraft during the LiDAR acquisition, providing high resolution imagery over the focus area. The ground pixel size of those images is about 15cm. The aerial image of the site was rectified for the purpose of providing ground reference data. The rectification was carried out by measuring corresponding points in the aerial photo and shaded relief generated from the LiDAR data (with 25 cm pixel size) and by transforming the aerial photo to match the shaded relief. The rectified image was used to estimate the percent cover of orange trees in the study area.

4. Methods

The transmitted and received LiDAR waveforms were decomposed using a custom Gaussian decomposition procedure with a trust-region-reflective optimisation algorithm according to Fieber *et al.* (2013a). The procedure was aimed at detecting weak pulses and obtaining a more complete vegetation structure. The decomposition provided point clouds with XYZ coordinates and additional parameters such as location of the pulses, their widths and backscattering coefficients.

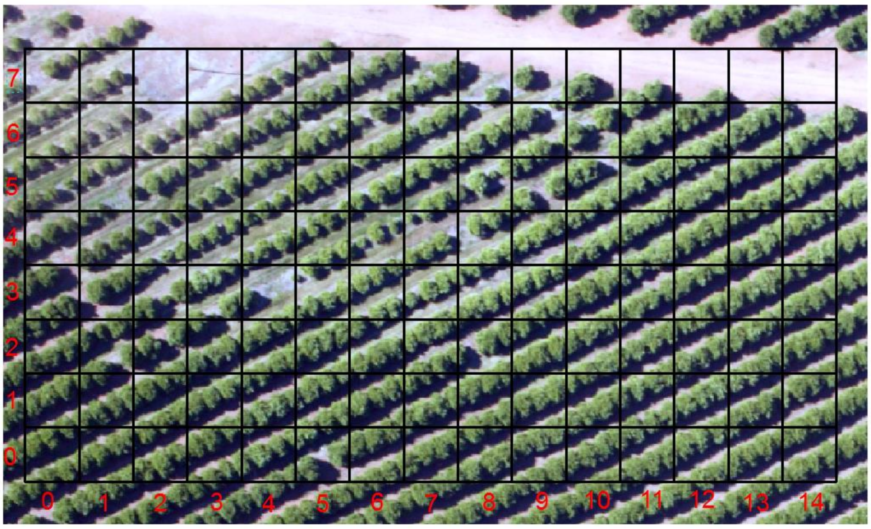

Figure 2. Orange orchard site with 10m by 10m grid overlaid.

4.1 Effective LAI retrieval from LiDAR

Effective Leaf Area Index (LAI_e) from LiDAR data was extracted in two ways: (i) from the raw waveforms as one of the stages in the Canopy Height Profile methodology (Harding *et al.*, 2001) adapted to small-footprint LiDAR data (Fieber *et al.*, 2013b) - Waveform method; as well as (ii) from gap probability calculated form decomposed point clouds - Discrete point method. The probability (P) of pulses reaching the ground without being intercepted in discrete point method was computed as the number of single ground returns (elevation<0.5 m) to the total number of waveforms incident on the area of interest. The vegetation-ground reflectance ratio used in the waveform method was constant and set to 0.5 for laser wavelength of 1550 nm. Both methods were previously validated against hemispherical photography in a heterogeneous forest site in the Murrumbidgee catchment and are described in Fieber *et al.* (2013b).
Effective LAI estimates were extracted for the whole orange orchard site, as well as in 2.5m by 2.5m, 5m by 5m, 10m by 10m, 30m by 20, and 50m by 40m grids using both LiDAR methods. Figure 2 shows the orange orchard test site with the 10 m grid overlaid. LAI_e in grids was then

summed up and averaged for the whole site. As a result of gridding estimation of LAI_e for a few cells in the smallest grid saturated due to its logarithmic transformation to account for occlusions. This means that none of the points in the grid cell reached the ground. In that case to enable calculation of site mean LAI_e for the whole site, the maximum LAI_e value in that particular grid was found prior to averaging and assigned to all saturated cells in the dataset.

4.2 Simulation of effective LAI values

The percentage of the test area covered by orange trees was estimated from manually generated land cover map by delineation of the tree crowns. The area of orange trees was estimated as 5898.4 m resulting in 49.15% tree cover of the study area (A_T). This information was used to calculate an estimate of single tree LAI_e from whole study area and gridded datasets - the overall LAI_e was divided by the tree covered fraction. Subsequently, to test the effects of vegetation discontinuity on LAI_e estimation, the values of effective LAI for the whole study area were simulated based on a set of increasing single orange tree LAI_{eT} (from 0.2 to 5 with 0.2 increments) and known vegetation (A_T) and ground (A_G=1-A_T) cover in the test area. This was done by predicting the LAI_e of the orange tree covered area and averaging it with the effective LAI of the bare soil area ($LAI_{eG} = 0$).

$$LAI_{eSITE-A} = \frac{LAI_{eT}A_T + LAI_{eG}A_G}{A_T + A_G} \tag{1}$$

These 'average' $LAI_{eSITE-A}$ values were compared to the 'overall' $LAI_{eSITE-O}$ calculated for the whole study area from summed probabilities of penetration for the orange tree area (P_{gapT}) and ground area (P_{gapG}=1).

$$LAI_{eSITE-O} = -\ln(\frac{P_{gapT}A_T + P_{gapG}A_G}{A_T + A_G}) \tag{2}$$

5. Results and discussion

5.1 Gridding impact on LAI retrievals

A summary of mean study area LAI_e values is presented in Table 1 and Figure 3 illustrates the gridding effect on LAI_e retrievals. The LAI_e derived using point method is usually higher than the waveform one by 5-10. This is consistent with the findings of Fieber *et al.* (2013b) where waveform method slightly underestimated and point method considerably overestimated hemispherical LAI_e.The only exception is the smallest grid where point LAI_e is lower than waveform LAI_e. The reason for this is that point LAI_e is limited by the density of LiDAR points which does not take into account the intensity of pulses. As a result the maximum LAI_e derived using point method does not exceed 3.5 whereas the maximum waveform LAI_e reaches about 9 when 2.5m grid is used (Figure 3, bottom row).

Table 1. Summary of mean site LAI_e values depending on the method and grid cell size used

Grid size	*Waveform LAI_e*	*Point LAI_e*	*Difference*
Whole orchard site	0.703	0.739	5.1%
50m by 40m grid	0.707	0.761	7.6%
30m by 20m grid	0.726	0.777	7.0%
10m by 10m grid	0.739	0.794	7.4%
5m by 5m grid	0.804	0.879	9.3%
2.5m by 2.5m grid	1.329	1.255	-5.6%

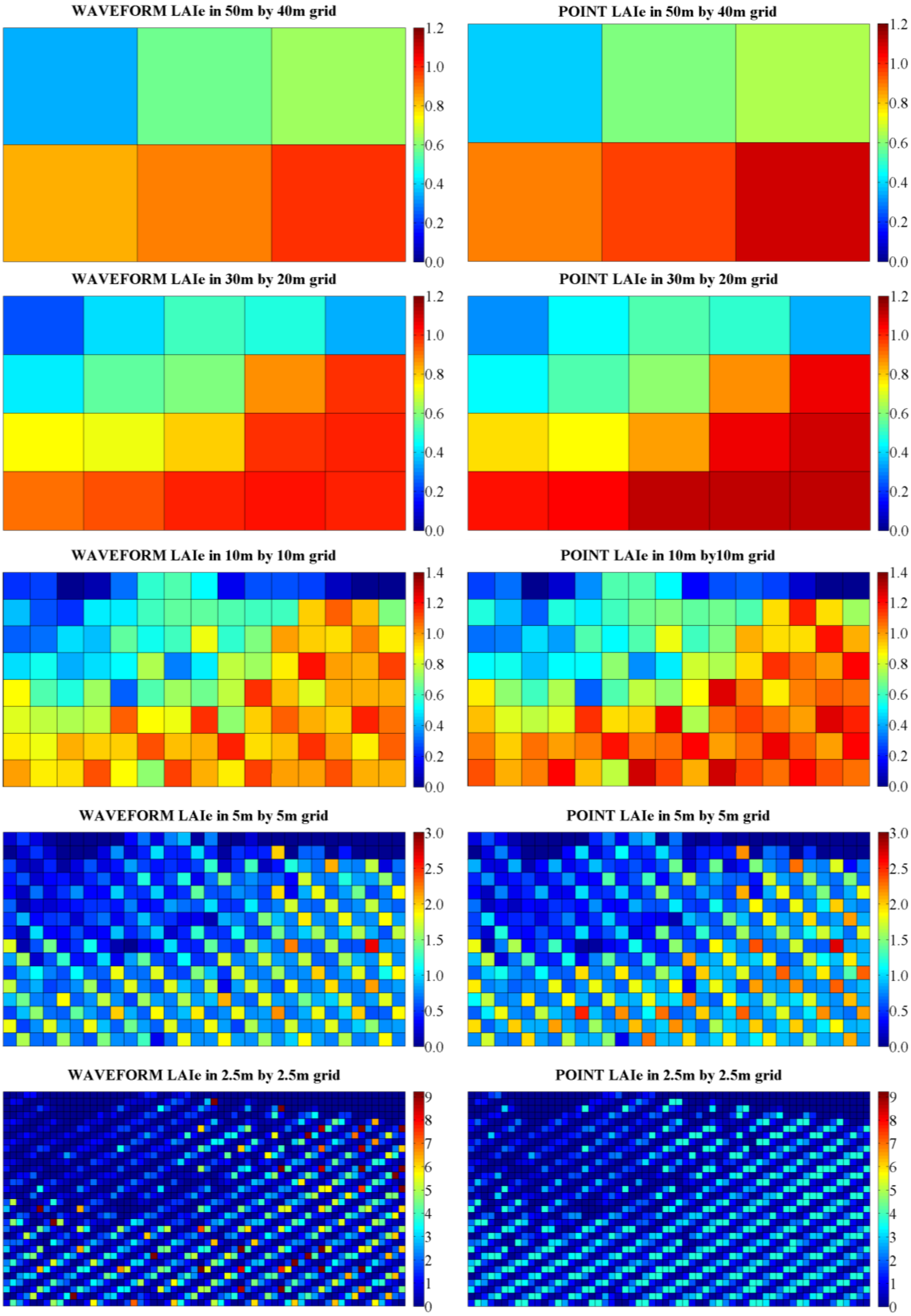

Figure 3. Effective leaf area index maps of the study area depending on the grid cell size used. Left column: waveform method; Right: discrete point method.

Furthermore, reducing the grid cell increases the overall LAI_e estimate as the cells include more homogenous land cover. As a result, the difference between the LAI_e calculated for the whole study area as one block (0.70/0.74) and in the smallest grid of 2.5 m by 2.5 m (1.33/1.26) was almost 90% for waveform and 83% for point method respectively. The smallest grid is not, however, ideal and it most likely overestimates the LAI_e of the whole study area. This may be due to the fact that such a small grid cell does not cover the area of a single tree crown, resulting in some cells not having ground returns, therefore, undefined LAI_e. The grid of 5 m by 5 m, covering the crown of a typical orange tree, is more likely to provide more reliable estimate of this study area LAI_e (0.80/0.88) and is therefore considered as the most suitable. This estimate is still 14%/19% higher than the estimate for the whole study area treated as one block (0.70/0.74), when the gaps between the rows are not accounted for.

5.2 Simulation of LAI_e – between-tree gaps

Table 2 presents the estimates of a single tree effective LAI based on the fraction of the area covered by the vegetation. As in the case of study area LAI_e, estimated tree LAI_e from the waveform method is usually lower than that of the point method. The only exception is grid with 2.5 m cells. Finally, as already discussed, 5 m grid may be optimal for LAI_e estimation for this study site as it is similar to the size of the tree crowns. Furthermore, as shown in Fieber *et al.* (2013b) the waveform method seems to provide estimates closer to estimates base on fish-eye lens photography. Therefore, considering an average LAI_e value of a single tree in the study area to be 1.64 (as shown in Table 2 for 5 m by 5 m grid from waveform method), the simulated value $LAI_{eSITE\text{-}A}$ for the whole study area accounting for gaps with similar LAI_e (1.6) of a single tree is 0.79 (Table 3). This value is in close agreement with the estimate of LAI_e in 5 m by 5 m grid for the whole study area, equal 0.80, listed in Table 1.
Table 3 shows predicted LAI_e values of the whole site area as well as average of LAI_e of the area covered by trees and by ground depending on the LAI_e of a single orange tree. The difference in the LAI_e calculated using two methods increases with the increasing LAI of a single tree, ranging from 5% for a single tree LAI_e of 0.2 to -73% for a single tree LAI_e of 5. Figure 4 illustrates the effect of underestimation of LAI_e by ‘overall’ method in comparison to ‘average’ method.

Table 2. Single tree LAI_e estimates from two LiDAR methods with different grid cell sizes

Grid size	***Waveform LAI_e***	***Point LAI_e***
Whole orchard site	1.430	1.504
50m by 40m grid	1.438	1.549
30m by 20m grid	1.477	1.582
10m by 10m grid	1.504	1.615
5m by 5m grid	1.636	1.788
2.5m by 2.5m grid	2.704	2.553

Table 3. Predicted LAI_{eSITE} values of the study area based on assumed LAI_{eT} of a single tree using 'average'(Eq.1) and 'overall' (Eq.2) approach.

LAI_{eT}	LAI_{eG}	A_T	A_G	P_{gapT}	P_{gapG}	$LAI_{eSITE-O}$	$LAI_{eSITE-A}$	$(LAI_{eSITE-O} - LAI_{eSITE-A})/LAI_{eSITE-A}$
0.2				0.8187		0.093	0.098	-5.1%
0.4				0.6703		0.177	0.197	-10.1%
0.6				0.5488		0.251	0.295	-15.0%
0.8				0.4493		0.316	0.393	-19.7%
1.0				0.3679		0.372	0.492	-24.3%
1.2				0.3012		0.421	0.590	-28.7%
1.4				0.2466		0.463	0.688	-32.8%
1.6				0.2019		0.498	0.786	-36.7%
1.8				0.1653		0.528	0.885	-40.3%
2.0				0.1353		0.553	0.983	-43.7%
2.2				0.1108		0.575	1.081	-46.9%
2.4				0.0907		0.592	1.180	-49.8%
2.6	0	49.15%	50.85%	0.0743	1	0.607	1.278	-52.5%
2.8				0.0608		0.619	1.376	-55.0%
3.0				0.0498		0.629	1.475	-57.3%
3.2				0.0408		0.638	1.573	-59.5%
3.4				0.0334		0.645	1.671	-61.4%
3.6				0.0273		0.650	1.769	-63.3%
3.8				0.0224		0.655	1.868	-64.9%
4.0				0.0183		0.659	1.966	-66.5%
4.2				0.0150		0.662	2.064	-67.9%
4.4				0.0123		0.664	2.163	-69.3%
4.6				0.0101		0.667	2.261	-70.5%
4.8				0.0082		0.668	2.359	-71.7%
5.0				0.0067		0.670	2.458	-72.7%

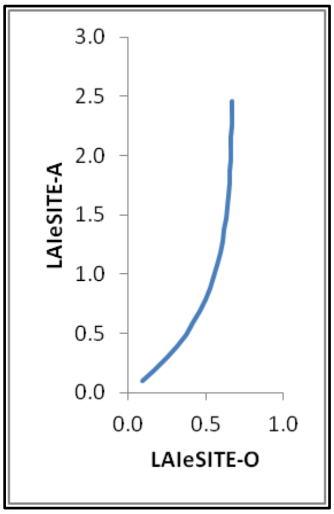

Figure 4. Underestimation of the LAI_e of the study area by 'overall' method (x axis) in comparison to 'average' method (y-axis).

6. Conclusions

Small-footprint laser scanning data offer the possibility of adjusting the aggregation area of LAI estimation to the site specifics. Aggregation to larger cells/cylinders needs to be performed due to the fact that small-footprint laser scanning data do not always have a ground return which in turn makes the calculation of LAI_e impossible owing to logarithmic transformation. Therefore, the grid cell size needs to be adjusted to the crown size of the trees in the study area to ensure that LAI_e values do not saturate. Small, site-adjusted grid sizes are however an important advantage in comparison to large-footprint data especially if the estimates are to be provided for a discontinuous canopy. This paper has presented a sensitivity study of LAI_e estimates from small-footprint full-waveform LiDAR data over a discontinuous orange orchard canopy to the grid cell size used. The difference in LAI_e estimated from a simulated large-footprint laser system covering the whole site and LAI_e estimated as the mean LAI_e value in 5m by 5 m grid was 14%. The gridded LAI_e estimate using a raw-waveform method agreed well with the simulated LAI_e value for the whole study area when a mean value of tree LAI_e and the row gap area was computed. This showed that the gridding approach to LAI_e estimation is a valid method and provides more reliable estimates than using large-footprint (large-aggregation area) data when the canopies are sparse or discontinuous. Furthermore, the simulation of LAI_e values as the average of tree LAI_e and LAI_e of bare soil area (soil LAI_e=0) ('average') and from summed probabilities of penetration for the orange tree area and ground area ('overall') showed that in the latter case underestimation of LAI_e can be very high (73% when LAI_e of a single tree is 5).

Acknowledgements

This work was funded by Engineering and Physical Sciences Research Council (grant number: EP/P505682/1), School of Mathematical and Physical Sciences and School of Systems Engineering of University of Reading. Field campaign data was funded by Australian Research Council projects LE0560930, DP0557543 and FS100100040. Waveform processing was funded by the National Centre for Earth Observation, UK.

References:

Black, T.A., Chen, J.-M., Lee, X., Sagar, R.M., 1991. Characteristics of shortwave and longwave irradiances under a Douglas-fir forest stand. *Canadian Journal of Forest Research*, 21 (7), 1020-1028.

Breda, N.J.J., 2003. Ground-based measurements of leaf area index: a review of methods, instruments and current controversies. *Journal of Experimental Botany*, 54 (392), 2403-2417.

Chen, J.M., Rich, P.M., Gower, S.T., Norman, J.M., Plummer, S., 1997. Leaf area index of boreal forests: Theory, techniques, and measurements. *Journal of Geophysical Research: Atmospheres*, 102 (D24), 29429-29443.

Fieber, K.D., Davenport, I.J., Ferryman, J.M., Gurney, R.J., Walker, J.P., Hacker, J.M., 2013a. Analysis of full-waveform LiDAR data for classification of an orange orchard scene. *ISPRS Journal of Photogrammetry and Remote Sensing*, 82 (0), 63-82.

Fieber, K.D., Davenport, I.J., Tanase, M.A., Ferryman, J.M., Gurney, R.J., Walker, J.P., Hacker, J.M., 2013b. Preliminary leaf area indes estimates from airborne small-footprint full-waveform lidar data. *International Geoscience and Remote Sensing Symposium IGARSS 2013*, Melbourne, Australia.

Harding, D.J., Lefsky, M.A., Parker, G.G., Blair, J.B., 2001. Laser altimeter canopy height profiles: methods and validation for closed-canopy, broadleaf forests. *Remote Sensing of Environment*, 76 (3), 283-297.

Lang, A.R.G., Yueqin, X., 1986. Estimation of leaf area index from transmission of direct sunlight in discontinuous canopies. *Agricultural and Forest Meteorology*, 37 (3), 229-243.

RIEGL, 2012. Riegl website. http://www.riegl.com (Accessed 9/11/ 2012).